Accurate Structure Determination of $Mo_6S_yI_z$ Nanowires from Atomic Pair Distribution Function (PDF) Analysis

Gianluca Paglia,[†,*] Emil S. Božin,[†] Damjan Vengust,[‡] Dragan Mihailovic,[‡,§,⊥] and Simon J. L. Billinge[†]

Department of Physics and Astronomy, Michigan State University, East Lansing, Michigan 48824-2320, Josef Stefan Institute, Jamova 39, SI-1000 Ljubljana, Slovenia, Faculty of Mathematics and Physics, University of Ljubljana, Jadranska 19, SI-1000 Ljubljana, Slovenia, and Mo6 d.o.o, Teslova 30, 1000 Ljubljana, Slovenia

Received August 15, 2005. Revised Manuscript Received October 19, 2005

The structure of the recently discovered systematically reproducible $Mo_6S_yI_z$ nanowires has been determined from the atomic pair distribution function (PDF) analysis of powder X-ray diffraction data. This total scattering approach was required because the nanowires are not perfectly crystalline and, therefore, the structure cannot be obtained crystallographically. Several nanotube and nanowire models were fit to the PDF data. The resulting best-fit model structure consists of nanowires of Mo_6 octahedra that are bridged by sulfur and terminated on the outside by iodine. This demonstrates the power of total scattering methods in accurately resolving structural issues in nanostructured materials where traditional crystallographic methods fail.

Introduction

Since the discovery of fullerenes and carbon nanotubes, there has been significant interest in making use of their remarkable properties to realize their wide range of potential applications. It has also been found that other inorganic compounds can form tubular and wirelike morphologies.[1−5] The ability to use nanometer-sized devices is dependent on the capability to reproduce them systematically on a large scale with tunable physical and functional properties. Unfortunately, the intrinsic inhomogeneity of bulk synthesized material and the difficulty in separating the as-synthesized material has hampered attempts to take full advantage of their properties.[6−8]

Recently, molybdenum-based nanowire materials with the general formula $Mo_xY_yX_z$ (Y = chalcogen, X = halogen)[4,7] were discovered and found to grow in bundles of identical nanowires that can be relatively easily dispersed in a variety of solvents to isolate the individual nanowires.[8] The ease of systematic production of these materials has resulted in rapid progress in investigations of the functional properties and applications. To date, it has been determined that these materials exhibit large Young's and small shear moduli,[6] which facilitate the potential use of these materials as ultralow-friction lubricants,[9] as strength-enhancing additives to composites,[8,10] and as easily processed field-emission tips.[11] They have also been observed to exhibit magnetic properties when doped with lithium[12] and are a candidate for hydrogen storage.[13] This range of properties has been obtained from using different synthesis stoichiometries to produce the nanowires.[7,8] From the literature, this observation seems to result in a variety of structural configurations and/or interstitial species.[4,7,8,14] However, detailed structural knowledge has not been obtained as rapidly, and this is a limiting factor in understanding and controlling the functional properties of these materials.

The original study of this material concluded it to be composed of (3,3) armchair single-walled nanotubes of MoS_2 with I atoms residing in interstitial trigonal voids between the tubes in the $P6_3$ space group.[4] This followed an earlier theoretical study that predicted the structure of MoS_2 nanotubes and investigated the variation in electrical proper-

* Author to whom correspondence should be addressed. E-mail: paglia@msu.edu.
† Department of Physics and Astronomy, Michigan State University.
‡ Josef Stefan Institute.
§ Faculty of Mathematics and Physics, University of Ljubljana.
⊥ Mo6 d.o.o.

(1) Tenne, R.; Margulis, L.; Genut, M.; Hodes, G. *Nature* **1992**, *360*, 444−446.
(2) Margulis, L.; Salitra, G.; Tenne, R.; Talianker, M. *Nature* **1993**, *365*, 113−114.
(3) Chopra, N. G.; Luyken, R. J.; Cherrey, K.; Crespi, V. H.; Cohen, M. L.; Louie, S. G. *Science* **1995**, *269*, 966−967.
(4) Remskar, M.; Mrzel, A.; Skraba, Z.; Jesih, A.; Ceh, M.; Demšar, J.; Stadelmann, P.; Lévy, F.; Mihailovic, D. *Science* **2001**, *292*, 479−481.
(5) Petkov, V.; Zavalij, P. Y.; Lutta, S.; Whittingham, M.; Parvanov, V.; Shastri, S. *Phys. Rev. B* **2004**, *69*, 085410.
(6) Kis, A.; Mihailovic, D.; Remskar, M.; Mrzel, A.; Jesih, A.; Piwonski, I.; Kulik, A. J.; Benoit, W.; Forro, L. *Adv. Mater.* **2003**, *15*, 733−735.
(7) Vrbanič, D.; Remskar, M.; Jesih, A.; Mrzel, A.; Umek, P.; Ponikar, M.; Jancar, B.; Meden, A.; Novosel, B.; Pejovnik, S.; Venturini, P.; Coleman, J. C.; Mihailovic, D. *Nanotechnology* **2004**, *15*, 635−638.
(8) Nicolosi, V.; Vrbanič, D.; Mrzel, A.; McCauley, J.; O'Flaherty, S.; Mihailovic, D.; Blau, W. J.; Coleman, J. C. *Chem. Phys. Lett.* **2005**, *401*, 13−18.
(9) Joly-Pottuz, L.; Dassenoy, F.; Martin, J. M.; D., V.; Mrzel, A.; Mihailovic, D.; Vogel, W.; Montagnac, G. *Tribol. Lett.* **2005**, *18*, 385−393.
(10) Nicolosi, V.; Vrbanič, D.; Mrzel, A.; McCauley, J.; O'Flaherty, S.; Mihailovic, D.; Blau, W. J.; Coleman, J. C. *J. Phys. Chem. B* **2005**, *109*, 7124−7133.
(11) Nemanic, V.; Zumer, M.; Zajec, B.; Pahor, J.; Remskar, M.; Mrzel, A.; Mihailovic, D. *Appl. Phys. Lett.* **2003**, *82*, 4573−4575.
(12) Dominko, R.; Arcon, D.; Mrzel, A.; Zorko, A.; Cevc, P.; Gabersceck, M.; Remskar, M.; Mihailovic, D. *Adv. Mater.* **2002**, *21*, 1531.
(13) Chen, J.; Wu, F. *Appl. Phys. A−Mater.* **2004**, *78*, 989−994.
(14) Meden, A.; Kodre, A.; Padežnick Gomilšek, J.; Arčon, I.; Vilfan, I.; Vrbanič, D.; Mrzel, A.; Mihailovic, D. *Nanotechnology* **2005**, *16*, 1578−1583.

10.1021/cm051833x CCC: $33.50
Published on Web 12/09/2005

ties as a function of tube diameter.[15] The synthesis techniques have evolved from using a catalyzed transport method[4] for producing the molybdenum-based nanowires to a more efficient procedure that involves direct synthesis from the individual elements.[7] With these developments, the view of the structural configuration has changed from that presented previously to that of a nanowire structure similar to that found in Chevrel phases.[7,14] However, unlike the well-ordered Chevrel phases,[16] these molybdenum-based nanowires are arranged incoherently with respect to each other, making structure solution difficult.

X-ray diffraction (XRD), which is the primary technique used to facilitate structural solutions, produces diffraction patterns that contain significant diffuse components. These characteristics arise because of the lack of long-range structural order that is inherent in highly crystalline periodic systems.[17] The recent work by Meden et al.[14] has provided insight into the skeletal structure of $Mo_6S_yI_z$ using Rietveld analysis of XRD data and extended X-ray adsorption fine structure (EXAFS) measurements. From an initial synthesis stoichiometry of $Mo_6S_3I_6$, they determined the stoichiometry to be $Mo_6S_{0.58}I_{8.46}$. However, their final structure yielded a weighted parameter, R_{wp}, of 15% from Rietveld analysis, which is large by Rietveld analysis standards.[18] This result is not surprising, given that the XRD pattern contains broad peaks and a large diffuse component, suggesting structural coherence at the nanometer-length scale.

It has recently been shown that the structure of such nanostructured materials can be elucidated through the use of atomic pair distribution function (PDF) analysis.[5,17,19,20] The atomic PDF is formally defined as

$$G(r) = 4\pi r(\rho(r) - \rho_o) \quad (1)$$

where $\rho(r)$ is the atomic-pair density, ρ_o the average atomic number density, and r the radial distance.[21] The PDF is the probability density of finding pairs of atoms separated by a distance r. It is obtained by a sine Fourier transformation of the reciprocal space total scattering structure function $S(Q)$, which is obtained from a diffraction experiment. This approach is widely used to study liquids and amorphous materials but has recently been successfully applied to nanocrystalline materials.[17] The advantage of using this technique over the traditional Bragg diffraction analysis is that it incorporates all components for the diffraction intensities; both Bragg and diffuse scattering contributions are considered equally, which is imperative when accurate structural information about poorly crystalline materials is required. Because the PDF produces quantitative information from materials that scatter diffusely, it is used here to assess the structure of $Mo_6S_yI_z$ nanowires.

Experimental Details

$Mo_6S_yI_z$ nanowires were obtained via direct synthesis from the elements, using a solution stoichiometry of $Mo_6S_3I_6$.[7] These samples were packed and sealed with Kapton tape in flat plate sample holders 1.0 mm thick. XRD data were collected using the recently developed rapid acquisition pair distribution function (RA-PDF) technique,[22] using an incident energy of 87.005 keV ($\lambda = 0.142479$ Å) at the 6-IDD beam line at the Advanced Photon Source (APS) at Argonne National Laboratory in Argonne, IL. A two-dimensional circular image plate camera (MAR345) 345 mm in diameter was mounted orthogonal to the beam with sample-to-detector beam path calibrated to be 208.857 mm. This procedure facilitates the collection of data in greatly reduced time. Instead of the average 8 h required to collect data using conventional X-ray measurement protocols, the RA-PDF procedure allows a data set to be collected in as little as 3 min. Here, three scans of 500 s each were performed. The multiple scans were performed to avoid detector saturation and to yield improved counting statistics. Using Fit2D,[23] the raw data sets obtained were averaged to improve the statistical accuracy and reduce any systematic error in the experimental setup, normalized with respect to the monitor counts, and then integrated to produce one-dimensional XRD data. The XRD pattern obtained for the nanowire sample is shown in Figure 1, which also displays the diffraction pattern for crystalline MoS_2 for comparison. The MoS_2 (Figure 1b) exhibited a lower background and well-defined Bragg peaks up to a high wave vector of $Q \approx 15-20$ Å^{-1} ($Q = 4\pi \sin(\theta/\lambda)$), which is due to the material being highly crystalline. By comparison, the $Mo_6S_yI_z$ nanowire sample contains fewer Bragg-like features and a considerably larger diffuse component. This is particularly evident when viewing the inset of Figure 1a, which shows the high-Q data on the same expanded scale as the inset in Figure 1b. Diffraction patterns such as that for the $Mo_6S_yI_z$ nanowires are characteristic of materials with nanoscale order.[17]

Generation of Pair Distribution Function (PDF) Data

It is important to ensure that the processed PDF data contains signal stemming solely from the sample.[24] Hence, data encompassing an empty sample holder and the scattering environment were collected for background subtractions. The total scattering function $S(Q)$, extracted from the total diffracted intensity according to

$$S(Q) = \frac{I^{coh}(Q) - \sum c_i |f_i(Q)|^2}{|\sum c_i f_i(Q)|^2} + 1 \quad (2)$$

where $I^{coh}(Q)$ is the measured scattering intensity and c_i and

(15) Seifert, G.; Terrones, H.; Terrones, G.; Jungnickel, M.; Frauenheim, T. *Phys. Rev. Lett.* **2000**, *85*, 146−149.
(16) Sergent, M.; Fischer, Q.; Decroux, M.; Perrin, C.; Chevrel, R. *J. Solid State Chem.* **1977**, *22*, 87.
(17) Billinge, S. J. L.; Kanatzidis, M. G. *Chem. Commun.* **2004**, 749−760.
(18) Note the agreement factor, R_{wp}, for the PDF fit is defined in ref 30. The definition is similar to that used in Rietveld analysis, but the functions being fit are significantly different. Hence, direct comparison of R_{wp} values from PDF and Rietveld analysis should not be made. R_{wp} values are a useful measure of the goodness of fit when comparing how different models fit to the same data. For Rietveld analysis, acceptable fits exhibit R_{wp} values of <5%. In contrast, fits to the PDF exhibit larger R_{wp} values than Rietveld fits. For well-crystallized samples, PDF R_{wp} values are typically 10%−20%. For example, fitting the correct structural model to the crystalline MoS_2 data shown here resulted in an R_{wp} value of ∼19%. For disordered materials, an R_{wp} value of 30% is still considered quite successful.
(19) Petkov, V.; Billinge, S. J. L.; Heising, J.; Kanatzidis, M. G. *J. Am. Chem. Soc.* **2000**, *122*, 11571−11576.
(20) Petkov, V.; Trikalitis, P. N.; Božin, E. S.; Billinge, S. J. L.; Vogt, T.; Kanatzidis, M. G. *J. Am. Chem. Soc.* **2002**, *124*, 10157.
(21) Warren, B. E. *X-ray Diffraction*; Dover: New York, 1990.
(22) Chupas, P. J.; Qiu, X.; Hanson, J. C.; Lee, P. L.; Grey, C. P.; Billinge, S. J. L. *J. Appl. Crystallogr.* **2003**, *36*, 1342−1347.
(23) Hammersley, A. P.; Svenson, S. O.; Hanfland, M.; Hauserman, D. *High-Pressure Res.* **1996**, *14*, 235−248.
(24) Egami, T.; Billinge, S. J. L. *Underneath the Bragg Peaks—Structural Analysis of Complex Materials*; Pergamon: Amsterdam, 2003.

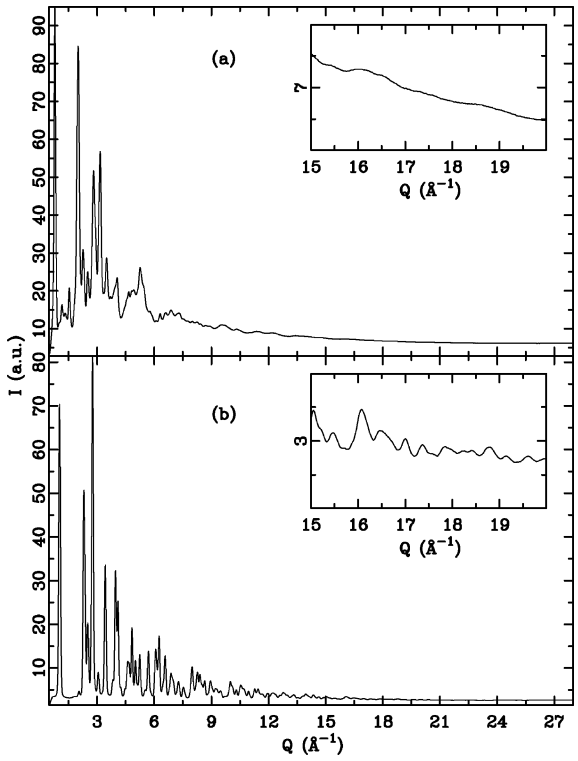

Figure 1. Experimental powder X-ray diffraction (XRD) patterns for (a) $Mo_6S_yI_z$ nanowires and (b) crystalline MoS_2, the latter of which is shown for comparison. Insets show amplified view of $I(Q)$ data at high Q.

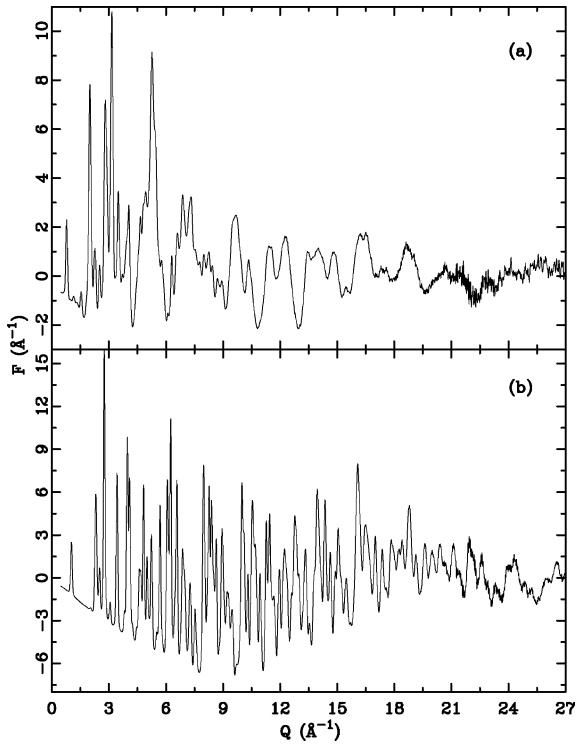

Figure 2. Experimental reduced structure functions for (a) $Mo_6S_yI_z$ nanowires and (b) crystalline MoS_2 shown for comparison.

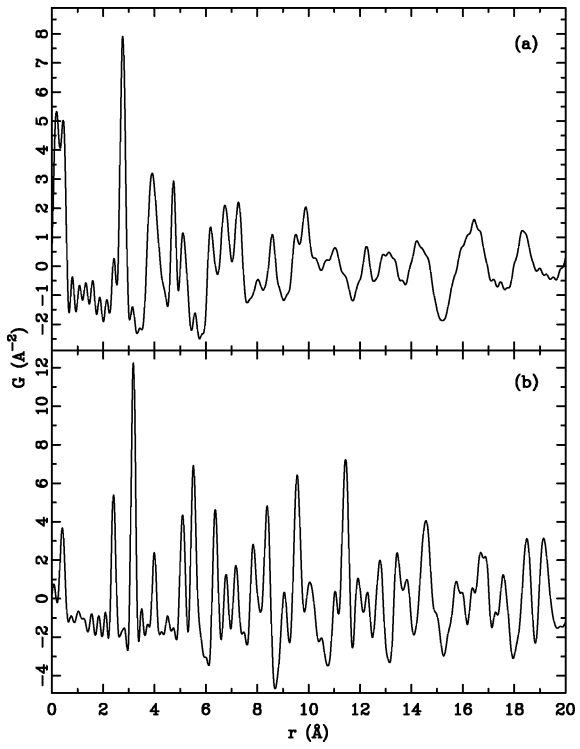

Figure 3. Experimental PDFs for (a) $Mo_6S_yI_z$ nanowires, and (b) crystalline MoS_2, the latter of which is shown for comparison.

$f_i(Q)$ are the atomic concentration and X-ray scattering factor, respectively, for atomic species i,[21,24] was derived for each sample. Both long-range atomic order represented by sharp Bragg peaks and local nonperiodic structural imperfections manifested in the diffuse components of the diffraction pattern are reflected in the $S(Q)$. It is convenient to represent the data in real space to facilitate simpler interpretation of the structural information. A Fourier transformation of the reduced total scattering structure function, $F(Q) = Q(S(Q) - 1)$, produces the real-space PDF:

$$G(r) = \frac{2}{\pi}\int_{Q_{min}}^{Q_{max}} Q[S(Q) - 1]\sin(Qr)\,dQ \qquad (3)$$

Here, Q is the magnitude of the wave vector, 2θ the angle between the incoming and outgoing radiation, and λ the wavelength of the X-ray radiation. The success of the PDF to provide fine structural details from disordered materials is dependent largely on the ability to access high Q values, typically >20 Å^{-1}. This can be achieved from most synchrotron and high-intensity neutron sources. For this experiment, the reduced structure functions, $F(Q)$, were truncated at $Q_{max} = 25$ Å^{-1}, before the PDF was calculated. Conversion of the XRD data to the scattering functions and PDFs was performed using PDFgetX2.[25]

The reduced structure functions and PDFs obtained are shown in Figures 2 and 3, respectively. The peaks in the PDF data below 2 Å are nonphysical and can be neglected. They originate from unavoidable systematic errors in the data arising from noise at high Q and termination effects due to the finite Q_{max} used. They are shown for the purpose of gauging the quality of the PDF and can be seen to die out to the level of the noise before the first physical peak (Mo−S) at 2.43 Å. Comparison between the data in Figures 1−3 illustrates why this approach yields quantitative local structural information in nanostructured materials. First, the data-reduction step to obtain $F(Q)$ results in an amplification of the important diffuse signal at high Q, which provides

(25) Qiu, X.; Thompson, J. W.; Billinge, S. J. L. *J. Appl. Crystallogr.* **2004**, *37*, 678.

critically important information about the local structure. This is somewhat neglected in the XRD pattern of $Mo_6S_yI_z$ (Figure 1a), which is dominated by strong Bragg peaks at low Q, and illustrates how traditional XRD is predominantly sensitive to long-range order. In the case of the crystalline MoS_2 the sharp Bragg features throughout the XRD pattern translate to much-sharper features in the $F(Q)$, giving it a spectrum that is characteristic of highly crystalline materials.

These amplified features of the $F(Q)$ are transferred into the real-space PDF, which contains far more directly measurable features than the original XRD patterns. Thus, the resulting PDFs are often sharp, well-defined functions in real space.[19,26] Hence, the enhanced sensitivity to the local atomic ordering in the PDF makes it well-suited for the structure determination of materials with limited structural coherence. After the PDF is obtained, an approach similar to Rietveld analysis[27] can be followed.[28] The effectiveness of this method of solving the structures of disordered materials has been demonstrated previously.[17,19,29]

Results and Discussion

The PDF allows us to comment directly on the order within the structure. Despite having significantly broadened diffraction patterns (compare Figures 2a and 2b), the $Mo_6S_yI_z$ nanowires yield sharp features in the PDF (Figure 3), making it a useful function for examining nanostructures. This is evident here with relatively sharp peaks in the $Mo_6S_yI_z$ PDF in the region below 12 Å, indicating a well-ordered local stucture, compared to a total structure that exhibits limited structural coherance, as discussed below. However, it should be noted that the peaks in the region are not as sharp as those in the equivalent region of the highly crystalline MoS_2 PDF, suggesting that there is some structural disorder on the local atomic scale. This region is dominated primarily by atomic interactions within individual nanowires. Interactions between neighboring nanowires contribute to the signal in the region of the PDF above the shortest interwire atom−atom distance of ∼4 Å, although they do not become dominant until higher r values. The first Bragg peak from the XRD data (Figure 1a), at $Q = 0.7841$ Å^{-1}, indicates a nanowire spacing of ∼8 Å. Examination of the Meden et al[14] model shows the center−center distance between nanowires to be 9.45 Å. The nearest-neighbor distance between terminal atoms of neighboring nanowires was ∼4 Å. Beyond 10 Å in the $Mo_6S_yI_z$ PDF, the peaks become increasingly broad, reflecting the poor ordering of the nanowires, but also indicating that the material has limited structural coherence along the length of individual nanowires and suggesting that the wires are not perfectly straight in the structure. The electron microscopy images[7,14] indicate the nanowires exhibit some curvature on the micrometer-length scale, which contributes to the long-range structural incoherance. Such curvature necessarily results in interwire disorder, similar to the turbostratic interlayer disorder observed in nanoparticulate V_2O_5.[20] If the bending is mild on the nanometer-length scale (as it is here), the aforementioned effect may be limiting the structural coherance.

To determine the structure of the $Mo_6S_yI_z$ nanowires, several models were fit to the experimental PDF and the parameters were refined to obtain the best agreement to the data using PDFFIT.[30]

Several structural analogues were attempted following the initial suggestion that the structure was that of a (3,3) armchair MoS_2 nanotube with interstitial I atoms stacked according to the $P6_3$ space group.[4] MoS_2 nanotubes have been considered as a two-dimensional (2D) layer of MoS_2 from the crystalline model conformally mapped against the surface of a cylinder to form a tube.[15] In the present case, this was approximated by assuming a fragment of the nanotube which consists of two MoS_2 layers separated by a distance representing the presumed tube diameter; this is an approach that has been used successfully by Petkov et al.[5] in the case of V_2O_5 nanotubes. The models that have been tested incorporated various tube diameters and were refined against the PDF data under $P1$ symmetry. The diameters ranged from 10 Å, as suggested by the data in the Remskar et al. study,[4] to 20 Å, which was suggested by Seifert et al.[15] to result in a tube of minimal energy. The nearest-neighbor Mo−S and Mo−Mo distances in these models were approximately consistent with those determined from EXAFS by Meden et al.,[14] at 2.43 and 2.68 Å, respectively. Iodine was incorporated into the models in two ways. Initially, it was inserted interstitially, as originally suggested,[4] both on the inside and outside of the tube. The distance at which I atoms were placed from Mo atoms in the starting models ranged from 3.15 to 2.78 Å, with the latter distance being the value determined from EXAFS.[14] The second manner in which I atoms were incorporated into the models was by substituting them for Mo and S atoms in the MoS_2 triple layers until the synthesis stoichiometry of $Mo_6S_3I_6$ was achieved, with the Mo−I distance being set at 2.78 Å in the starting model. The stoichiometry was also varied for several of the refinement trials, to allow for different possible compositions. None of these series of models provided a successful refinement to the data. The refinement fits proved unreasonable, often producing negative scale factors, and only became semi-reasonable below $r < 15$ Å at the expense of the structural integrity of the models. The best refinement obtained is shown in Figure 4a, exhibiting an R_{wp} value of 52.5%.

A second type of structural model was composed of a full single-layered (3,3) $Mo_6S_3I_6$ nanotube with a repeat length of 9 Å. Refinement of this model to the PDF provided a reasonable fit that reproduced the main features at $r < 10$ Å quite well (Figure 4b). The best achieved R_{wp} value was 39.7%. While the model maintained an approximate nanotube configuration, it was observed that the Mo−S, Mo−Mo, and Mo−I distances did not closely reflect the EXAFS measured values of Meden et al.[14] Furthermore, most of the parameters

(26) Peterson, P. F.; Proffen, Th.; Jeong, I.-K.; Billinge, S. J. L.; Choi, K.-S.; Kanatzidis, M. G.; Radaelli, P. G. *Phys. Rev. B* **2001**, *63*, 165211.
(27) Rietveld, H. M. *J. Appl. Crystallogr.* **1969**, *2*, 65.
(28) Billinge, S. J. L. In *Local Structure from Diffraction*; Billinge, S. J. L., Thorpe, M. F., Eds.; Plenum Press: New York, 1998; p 137.
(29) Petkov, V.; Billinge, S. J. L.; Vogt, T.; Ichimura, A. S.; Dye, J. L. *Phys. Rev. Lett.* **2002**, *89*, 075502.
(30) Proffen, Th.; Billinge, S. J. L. *J. Appl. Crystallogr.* **1999**, *32*, 572−575.

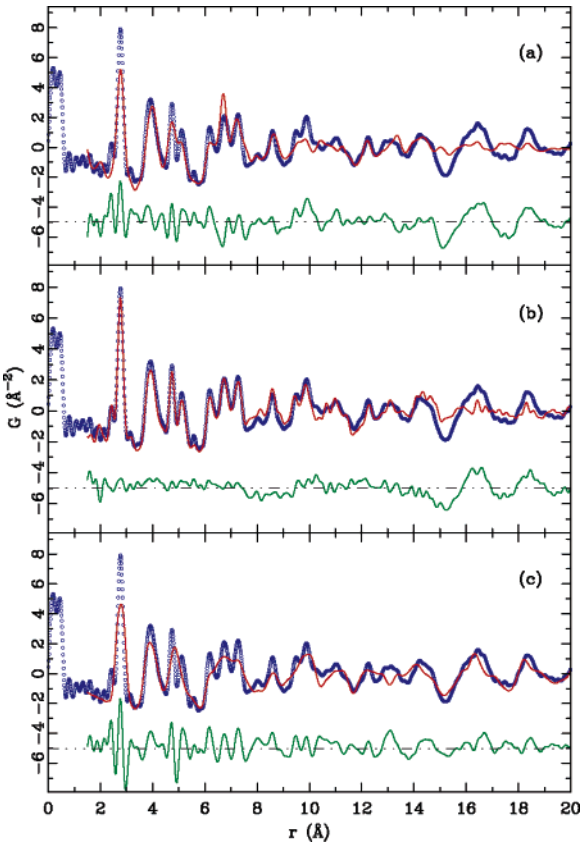

Figure 4. Refinement fits of calculated atomic pair distribution functions (PDFs) (solid line) against $Mo_6S_yI_z$ nanowire data (circles) for (a) the best fit from model trials incorporating nanotube walls based on triple layers of MoS_2, (b) single-layered (3,3) $Mo_6S_3I_6$ nanotube model, and (c) nanowire model of Meden et al.,[14] based on the Chevrel phases. The solid line below each PDF is the difference between the experimental and calculated PDFs.

exhibited large correlations during the refinement. As a result, the possibility of the $Mo_6S_yI_z$ nanowires exhibiting a single-layered nanotube topology was discounted.

Meden et al.[14] proposed, from complementary use of EXAFS and XRD, that the $Mo_6S_yI_z$ nanowire topology is similar to that of the Chevrel phases[16] with octahedra of six Mo ions (Mo_6) forming the building blocks of the wire that are bridged together by partially occupied S sites and terminal positions of the wire occupied by both S and I atoms. They determined the structure to be independent of the synthesis stoichiometry, with the final model having a very low sulfur content, with a stoichiometry of $Mo_6S_{0.58}I_{8.46}$. The structural model is described using $P6_3$ space group symmetry and contains shared occupancy between S and I atoms on most of the terminal sites of the nanowires. Refinement of the model against the PDF data was performed initially with the internal parameters fixed and resulted in the relatively poor fit shown in Figure 4c, yielding a large R_{wp} of 50.4%.[18] Thermal parameters had a tendency to become negative during the refinement, particularly for the S atoms. Attempts to refine the internal parameters proved difficult and resulted in significantly higher R_{wp} values. However, the peak shapes of the calculated PDF were qualitatively determined to match the data over the entire range, which was not the case for the other trial models shown in Figures 4a and 4b. The high R_{wp} value obtained from the fitting of the Meden et al.[14] model to the PDF data is not surprising, given that it was derived from a Rietveld analysis of the XRD data, which results in the consideration of the Bragg scattering component alone while the diffuse component is ignored. This implies that the Meden et al.[14] model represents an somewhat idealized structural model of the $Mo_6S_yI_x$ nanowire topology.

Therefore, it was decided to pursue the Meden et al.[14] model further to obtain an accurate structural model. The observation of negative thermal parameters for S atoms and the relative instability when attempting to refine the internal parameters suggests that some atom species should be positioned in different locations. Possible atom configurations were examined by taking individual nanowires of varying atom composition and refining them against the PDF data under $P1$ symmetry to a maximum r range of 10 Å. The approach adopted was to keep the Mo_6 octahedra fixed to maintain the basic framework of the nanowire while refining the anion species iteratively, in groups of four per iteration, until the minimum R_{wp} value was obtained. A description of the trial configurations examined, their resulting refinement R_{wp} values, and a summary of the key observations is given in Table 1. With the exception of trial 4, all anions were assigned to fully occupy their designated site positions. In all cases, after the anion species were refined, the molybdenum was allowed to refine, to determine whether its octahedral configuration was maintained. This was observed to be the case, with the R_{wp} values significantly reduced to values of <10%. In the case of trial 4, where the I and S atoms were set to partially occupy all site positions to comply with the $Mo_6S_3I_6$ synthesis stoichiometry, the occupancy was incorporated into the refinement after the anions were refined. An example of the trial nanowire structures is illustrated in Figure 5a.

All the refinements described in Table 1 reproduced the features of the PDF well and resulted in good R_{wp} values. Trial 4 resulted in the highest R_{wp} values obtained, whereas trial 2 produced the best statistical fit to the data. Trials 1

Table 1. Summary of Trial Refined Atom Configurations for Individual Nanowires and Resulting R_{wp}

trial number	configuration	comments	R_{wp}[a] (%)
1	$Mo_6S_3I_6$ stoichiometry. Both I and S occupy terminal positions. Also, both I and S trialed in bridging positions between the Mo_6 octahedra.	S migrates away from nanowire when refined. Bridging I migrates away from nanowire (S does not). − indicates S is bridging.	16.0
2	Only I occupying terminal positions, S occupying bridging positions.	Best fit, all atoms at physically reasonable distances.	15.8
3	Only I in nanowire, no S.	Bridging I migrates away from nanowire.	16.4
4	Virtual Crystal. I and S set to partially occupy all anion sites according to $Mo_6S_3I_6$ stoichiometry.	S occupancy becomes very small (<0.08) when refined.	19.6

[a] Weighted Rietveld agreement factor. See ref 18 for comments.

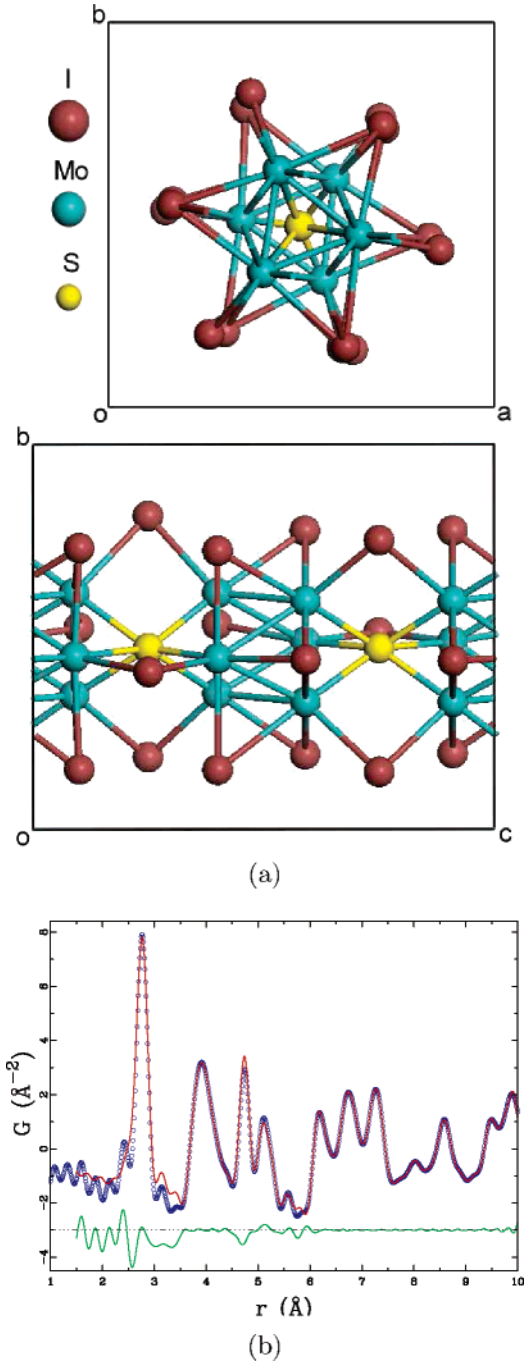

Figure 5. (a) Pictorial representation of the individual nanowires used to assess possible configurations of the $Mo_6S_yI_z$ structure. In this case, the trial 2 configuration is shown. (b) Resulting refinement fit of calculated PDF (solid line) against $Mo_6S_yI_z$ nanowire data (circles) for the trial 2 structure. The solid line below the PDF is the difference between the experimental and calculated PDF.

and 4 both indicated that sulfur does not lie in the terminal positions of the nanowire but rather is centrally located in the wire. In the case of trial 4, a refinement of the occupancies resulted in a very small refined occupancy of the S atoms (<0.08), suggesting that sulfur may not reside in the nanowire. For trial 1, the S atoms that were occupying terminal positions in the nanowire migrated away to unreasonable distances from the Mo_6 octahedra during the refinement, suggesting that they may reside interstitially between neighboring nanowires. Also, for trial 1, when refinements were conducted with I atoms placed in the bridging positions

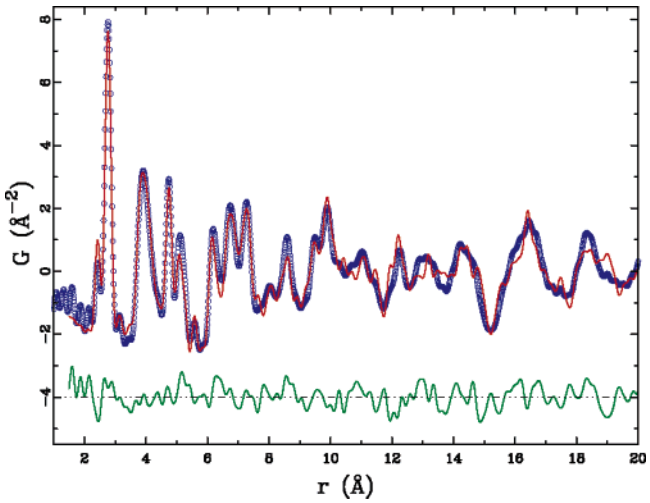

Figure 6. Resulting refinement fit of calculated PDF (solid line) against $Mo_6S_yI_z$ nanowire data (circles) for the full unit-cell model with I atoms occupying only the terminal positions of the nanowires and S atoms only occupying bridging positions between the Mo_6 octahedra.

between the Mo_6 octahedra, they migrated away from the nanowire. However, when S atoms were refined in the bridging positions, they remained in place. Trial 3 also exhibited iodine that was placed in bridging positions migrating away from the nanowire during refinement. In all cases, I atoms placed in terminal positions along the nanowire remained at physically reasonable distances. Therefore, of all the trial structures, that of Trial 2 maintained the best physical integrity of the nanowire structure with the terminal iodines remaining at physically reasonable distances from the Mo_6 octahedra and the two bridging S atoms remaining in place. This configuration, along with its fit to the PDF data is shown in Figure 5. It is thus concluded that the nanowires are composed of Mo_6 octahedra bridged by S anions, with all terminal positions being occupied by I atoms. Having S atoms occupy only bridging positions results in an occupancy of 0.0625, which agrees with the result from the trial 4 virtual crystal refinements. This low occupancy of the sulfur is also supported directly by the relative intensities of the peaks in the PDF (Figure 5b). The Mo−Mo and Mo−I distances of 2.68 and 2.78 Å, determined from EXAFS,[14] are represented by a large broad peak centered at 2.76 Å in the PDF. The Mo−S distance, as determined by EXAFS,[14] is 2.43 Å. The peak corresponding to this distance in the PDF is <10% as intense as that at 2.76 Å and, therefore, suggests a low sulfur content.

The trial 2 configuration was then incorporated into the full unit-cell model of Meden et al.[14] Refinement of this model resulted in a final R_{wp} value of 26.3%.[18] This represents a much-improved fit, compared to all the other structural analogues that were tried. The fit of this model is shown in Figure 6, and the refined structural parameters are summarized in Table 2. The major improvement in the model from that of Meden et al.,[14] in addition to the more precise determination of which sites the I and S atoms are situated in, is that the present model incorporates more distortion within each individual nanowire. The higher root-mean-square (RMS) displacements exhibited by the iodine species, signified by the higher thermal factors in Table 2, are partly

Table 2. Refined Parameters for the $Mo_6S_yI_z$ Structure[a]

Space Group $P6_3$, a, = 16.4100(1) Å, c = 11.9154(1) Å				
atom[b]	x	y	z	U(Å^2)
Mo	0.9042(2)	0.9178(3)	0.1486(2)	0.0007(1)
Mo	0.0942(2)	0.0709(2)	0.3147(1)	0.0007(1)
Mo	0.2296(1)	0.5760(3)	0.3482(1)	0.0007(1)
Mo	0.2381(3)	0.5950(2)	0.0563(2)	0.0007(1)
Mo	0.4240(1)	0.7429(2)	0.5293(4)	0.0007(1)
Mo	0.4338(3)	0.7489(3)	0.8591(3)	0.0007(1)
I	0.2135(3)	0.1885(3)	0.1530(3)	0.0024(2)
I	0.0452(3)	0.2118(2)	0.3317(3)	0.0024(2)
I	0.5407(3)	0.8490(3)	0.3595(4)	0.0024(2)
I	0.5539(3)	0.8463(3)	0.0369(3)	0.0024(2)
I	0.3737(2)	0.8693(1)	0.5995(2)	0.0024(2)
I	0.3701(3)	0.8790(3)	0.8659(2)	0.0024(2)
I	0.0286(3)	0.2288(2)	0.9983(4)	0.0024(2)
I	0.5309(1)	0.6196(4)	0.1820(3)	0.0024(2)
I	0.4288(1)	0.1370(1)	0.2217(3)	0.0024(2)
S[§]	0	0	0.0000	0.0006(1)
S[†]	1/3	2/3	0.2000	0.0006(1)
S[†]	1/3	2/3	0.7000	0.0006(1)

[a] All species have occupancies set to 1.00. S coordinates were not refined to fix the origin. [b] All Mo and I species occupy Wyckoff 6*c* positions, S[§] occupy 2*a* positions, and S[†] occupy 2*b* positions.

due to the varied Mo−I bond lengths in the final structural model. This highlights the structural disorder of the nanowires, even over dimensions as small as 2 nm. These experimental findings serve as independent evidence to exclude the possibility of a tubular structure in favor of a wirelike structure for $Mo_6S_yI_z$. It has also demonstrated how the atomic PDF, which is rich in well-defined structure-sensitive features reflecting the relative positions of atoms, allows for an accurate structure determination of spatially incoherent materials.

Conclusion

We have described the derivation of an accurate structural model for the $Mo_6S_yI_z$ nanowires using atom pair distribution function (PDF) analysis. The derived model is based on that of Meden et al.[14] The nanowires consist of Mo_6 octahedral building blocks bridged by S atoms that lie at the center of the wire. The Mo atoms are terminated on the outside of the wire by I atoms. These nanowires are approximately hexagonally packed, according to $P6_3$ space group symmetry, although the interwire order is poor. Because of the short structural coherence, which is due to the poor interwire packing and, presumably, curved shape of the nanowires, the structure could not be solved crystallographically, necessitating a local structural approach, such as the atomic PDF method used here. This demonstrates the power of total scattering methods in accurately resolving structural issues in nanostructured materials where traditional crystallographic methods fail.

Acknowledgment. We would like to thank Professors Valeri Petkov and Mercouri Kanatzidis for helpful discussions. We would also like to acknowledge the assistance of Dr. Didier Wermeille, Dr. Doug Robinson, Dr. Pavol Juhas, HyunJeong Kim, He Lin, Ahmad Masadeh, Moneeb Shatnawi, and Mouath Shatnawi for collecting the data. This work was supported by the National Science Foundation (NSF), through Grant No. CHE-0211029. The APS is supported by the United States Department of Energy (U.S. DOE), under Contract No. W-31-109-Eng-38. The MUCAT sector at the APS is supported by DOE Contract No. W-7405-Eng-82.

CM051833X